

Exciton quantum beats in GaAs/AlAs disk-shaped quantum dots

Le Thi Dieu Hien^{1,2}, Le Thi Ngoc Bao¹, Dinh Nhu Thao^{2*}

¹Hue University of Sciences, Hue University, 77 Nguyen Hue Street, Hue City, Vietnam

²Hue University of Education, Hue University, 34 Le Loi Street, Hue City, Vietnam

* Correspondence to Dinh Nhu Thao <dnthao@hueuni.edu.vn>

(Received: 22 August 2022; Accepted: 10 November 2022)

Abstract. Using the renormalized wavefunction approach, we examined the excitonic quantum beat in a three-level system in disk-shaped quantum dots. The non-stationary electron wave function and the time-dependent exciton absorption intensity under the effect of an intensity pump laser that resonates with two excited electron states were also provided. Our numerical findings demonstrate that the time-dependent exciton absorption intensity takes the shape of a periodic oscillation when the quantum dot is subjected to a powerful resonant pump laser. This is clear evidence that quantum beats appears in the quantum disk. Additionally, the dot radius and the pump field detuning significantly affect the beat characteristics, such as frequency and amplitude.

Keywords: exciton quantum beats, disk-shaped quantum dots, GaAs/AlAs

1 Introduction

Due to its exceptional and cutting-edge uses in optoelectronics and electronic devices, semiconductor quantum dots have recently caught the attention of scientists [1, 2]. Quantum dots may now be created in a variety of sizes and forms for use in research to clarify the unique qualities that other low-dimensional structures do not have, thanks to breakthroughs in microelectronics technology. A unique variety of quantum dot that can be thought of as a quasi-one-dimensional quantum wire is the disk-shaped semiconductor nanostructure. This structure has now been taken into consideration for distinct theoretical and experimental studies [3–8].

Since the 1990s, both experimental and theoretical researchers have been interested in the quantum beats (QBs) phenomena [9]. QBs in

nanostructured semiconductors play an important role in ultrafast physics and have implications in the production of Terahertz electromagnetic waves [10, 11] and ultrafast all-optical switches [12]. In addition, nuclear, atomic, and molecular spectroscopy [13] makes extensive use of the quantum beat effect. Theoretically, the QBs have been investigated using the third-order nonlinear susceptibility method [14], the density matrix technique [15], the renormalized wavefunction approach [16–19], the non-equilibrium many body perturbation theory [20], and the photoemission theory [21]. When studying quantum dots of various shapes, such as spherical quantum dots [17] and elliptical quantum dots [19], or in a variety of low-dimensional structures, such as quantum wells [16] and quantum wires [18], the renormalized wavefunction technique has proven to be advantageous.

The goal of the current research is to use the renormalized wavefunction method to investigate the quantum beat phenomena in a disk-shaped quantum dot. Investigations are also done into the ways the QBs behave and the manner in which the external field and dot size affect them. The structure of this work is as follows. In section 2, the theoretical framework is described. Section 3 contains the numerical results and explanations. In section 4, we finalize the conclusions.

2 Theoretical framework

2.1 The wavefunction and energy levels of exciton in a disk-shaped quantum dot under the effect of a pump laser

In this work, to study the existence of exciton quantum beat in disk-shaped quantum dots, we irradiate simultaneously two laser waves on the system. A resonant pump laser has a frequency tuned close to the energy difference between the first two excited levels of the exciton (as indicated by a thick arrow in Fig. 1). A weak probe laser is utilized to identify the transitions between the ground level and the excited levels of the exciton (as indicated by a thin arrow in Fig. 1). We assume that these laser waves are set to irradiate on the same area of the cross-section of the quantum disk. In addition, the propagation direction of the laser beams is also set along the Oz axis (Fig. 1). Since the direction of laser beams is parallel to the Oz axis, the electric fields of lasers stay in the plane perpendicular to the Oz .

To study the behavior of the exciton quantum beat in a disk-shaped quantum dot with an infinite potential, we applied the three-level energy model of electron and hole (Fig. 2a) for exciton. The three-level energy system of exciton consists of a ground level E_{ground} corresponding to the state $|0\rangle$, two excited levels E_{10} and E_{11} corresponding to two states $|\Lambda_{10}\rangle$ and $|\Lambda_{11}\rangle$

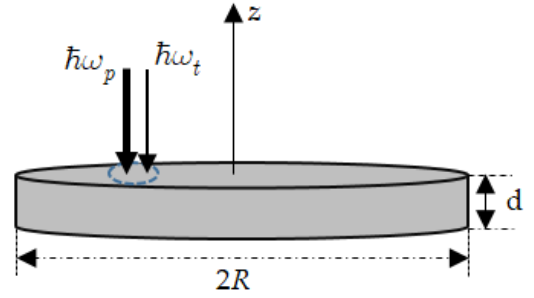


Fig. 1. The image illustrates the direction of the laser fields on the disk-shaped quantum dot

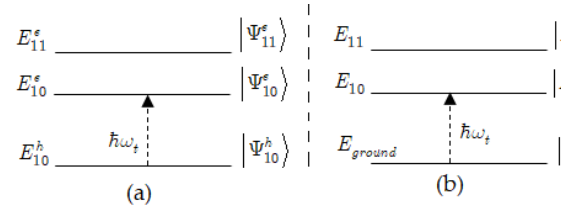


Fig. 2. (a) Model of the three-level electron system consists of the lowest level of the hole E_{10}^h and the two lowest levels of the electron E_{10}^e and E_{11}^e . (b)

A three-level model of the exciton consists of a ground level E_{ground} and two excited levels E_{10} và E_{11}

(Fig. 2b). These exciton states are achieved by interband optical transitions between the lowest level of the hole E_{10}^h and the two lowest levels of the electron E_{10}^e and E_{11}^e together with the Coulomb interaction among electrons and holes.

First, we find the wavefunction and energy spectrum of the exciton when the system is not affected by a pump laser. In the strong confinement regime, the time-dependent wavefunctions of exciton in the stationary state are given as follows

$$\begin{cases} \Lambda_{10}^h(\vec{r}, t) = \Lambda_{10}^h(\vec{r}, t) \Lambda_{10}^e(\vec{r}, t), \\ \Lambda_{11}^h(\vec{r}, t) = \Lambda_{10}^h(\vec{r}, t) \Lambda_{11}^e(\vec{r}, t), \end{cases} \quad (1)$$

where $\Lambda_{10}^h(\vec{r}, t)$, $\Lambda_{10}^e(\vec{r}, t)$, and $\Lambda_{11}^e(\vec{r}, t)$ are respectively the time-dependent wavefunctions of hole and electron, given as follows

$$\begin{cases} \Lambda_{10}^h(\vec{r}, t) = \Lambda_{10}^h(\vec{r})e^{-\frac{i}{\hbar}E_{10}^h t} = u_v \vec{r} \Psi_{10}^h \vec{r} e^{-\frac{i}{\hbar}E_{10}^h t}, \\ \Lambda_{10}^e(\vec{r}, t) = \Lambda_{10}^e(\vec{r})e^{-\frac{i}{\hbar}E_{10}^e t} = u_c \vec{r} \Psi_{10}^e \vec{r} e^{-\frac{i}{\hbar}E_{10}^e t}, \\ \Lambda_{11}^e(\vec{r}, t) = \Lambda_{11}^e(\vec{r})e^{-\frac{i}{\hbar}E_{11}^e t} = u_c \vec{r} \Psi_{11}^e \vec{r} e^{-\frac{i}{\hbar}E_{11}^e t}, \end{cases} \quad (2)$$

where $u_{c,v} \vec{r}$ are the periodic Bloch function located near the center of the Brillouin zone in the conduction and valence bands; $\Psi_{nm}^{e,h} \vec{r}$ is the envelope wavefunction of electron and hole in a disk-shaped quantum dot with an infinite potential [8]

$$\Psi_{nm}^{e,h}(\vec{r}) = \sqrt{\frac{2}{\pi d R^2}} \frac{1}{J_{m+1}(\chi_{nm})} \times J_m\left(\chi_{nm} \frac{r}{R}\right) \sin \frac{n_z \pi z}{d} e^{im\varphi}, \quad (3)$$

in which χ_{nm} is the n th zero of the m th order Bessel function of the first kind $J_m(\chi_{nm} \frac{r}{R})$.

If we choose the energy origin at the top of the valence band, the electron and hole energy levels corresponding to the wavefunctions in Eq. (3) are given by

$$\begin{cases} E_{nm}^e = E_g + \frac{\hbar^2 \chi_{nm}^2}{2m_e^* R^2} + \frac{n_z^2 \pi^2 \hbar^2}{2m_e^* d^2}, \\ E_{nm}^h = \frac{\hbar^2 \chi_{nm}^2}{2m_h^* R^2} + \frac{n_z^2 \pi^2 \hbar^2}{2m_h^* d^2}, \end{cases} \quad (4)$$

where E_g is the band gap energy of the semiconductor.

The energy levels of the exciton corresponding to the stationary states in Eq. (1) are determined as

$$\begin{cases} E_{10} = E_{10}^h + E_{10}^e, \\ E_{11} = E_{10}^h + E_{11}^e, \end{cases} \quad (5)$$

note that the binding energy between the electron and the hole is too small comparing to the electron and hole energy so we can ignore this value in Eq. (5).

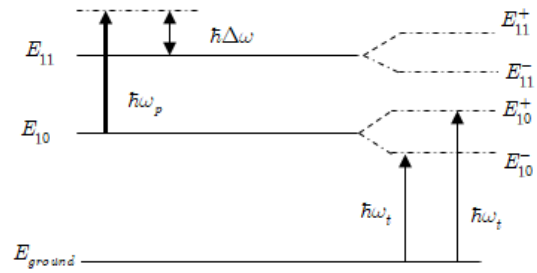


Fig. 3. Energy separation diagram of the exciton under the effect of a strong pump laser resonating with the energy difference between the two levels of the electron.

Next, we give the wave function and energy spectrum of exciton when the system is affected by a strong pump laser resonating with the difference between the two initial excitation levels of the electron. First, the wavefunction of the electron in the non-stationary state under the effect of a pump laser is determined from the time-dependent Schrödinger equation

$$i\hbar \frac{\partial \Lambda_{mix}^e(\vec{r}, t)}{\partial t} = (\hat{H}_0 + \hat{H}_{int}) \Lambda_{mix}^e(\vec{r}, t), \quad (6)$$

where \hat{H}_0 is the Hamiltonian without the pump laser and \hat{H}_{int} is the interaction Hamiltonian between the particles and the electromagnetic field of the pump laser, given as follows

$$\hat{H}_{int} = -\frac{q}{m_0} \frac{A_x e^{-i\omega_x t}}{i\omega_x} \vec{n} \hat{p} \equiv V e^{-i\omega_x t}, \quad (7)$$

in which the polarization vector \vec{n} is chosen along the Ox axis because the direction of the laser waves is parallel to the Oz axis (Fig. 1), $x = p$ and $x = t$ represent the pump and probe lasers, respectively; A_x and ω_x are the amplitude and frequency of laser waves, respectively.

Substituting Eq. (7) into Eq. (6), we can find the renormalized wavefunction of the electron in the presence of a pump laser as follows

$$\Lambda_{mix}^e(\vec{r}, t) = \frac{1}{2\Omega_R} \left(\alpha_1 e^{-\frac{i}{\hbar} E_{10}^- t} + \alpha_2 e^{-\frac{i}{\hbar} E_{10}^+ t} \right) \Lambda_{10}^e(\vec{r}) - \frac{V_{10}}{2\hbar\Omega_R} \left(e^{-\frac{i}{\hbar} E_{11}^- t} - e^{-\frac{i}{\hbar} E_{11}^+ t} \right) \Lambda_{11}^e(\vec{r}), \quad (8)$$

When the pump laser is activated, the electrons are now in a non-stationary state, causing the time-dependent wave function of the exciton being renormalized and determined by

$$\Lambda_{mix}(\vec{r}, t) = \Lambda_{10}^h(\vec{r}, t) \Lambda_{mix}^e(\vec{r}, t), \quad (9)$$

Substitute Eqs. (2) and (8) into Eq. (9) and perform some intermediate calculations, we obtain the renormalized exciton wavefunction expression of the following form

$$\Lambda_{mix}(\vec{r}, t) = \frac{1}{2\Omega_R} \left(\alpha_1 e^{-\frac{i}{\hbar} E_{10}^- t} + \alpha_2 e^{-\frac{i}{\hbar} E_{10}^+ t} \right) \Lambda_{10}(\vec{r}) - \frac{V_{10}}{2\hbar\Omega_R} \left(e^{-\frac{i}{\hbar} E_{11}^- t} - e^{-\frac{i}{\hbar} E_{11}^+ t} \right) \Lambda_{11}(\vec{r}), \quad (10)$$

where

$$\left\{ \begin{array}{l} \Omega_R = \left[\frac{\Delta\omega^2}{4} + \frac{|V_{10}|^2}{\hbar^2} \right]^{1/2} \\ \alpha_1 = \Omega_R - \frac{\Delta\omega}{2} \\ \alpha_2 = \Omega_R + \frac{\Delta\omega}{2} \\ \Delta\omega = \omega_p - \frac{E_{11}^e - E_{10}^e}{\hbar} \end{array} \right., \quad (11)$$

with V_{10} is the intraband transition matrix element between two levels E_{10}^e and E_{11}^e

$$V_{10} = \frac{q}{m_0} \frac{A_p}{i\omega_p} \frac{m_e}{i\hbar} \frac{E_{11}^e - E_{10}^e}{J_1(\chi_{10})J_2(\chi_{11})} \frac{R}{1} \times \int_0^1 J_0(\chi_{10}r) J_1(\chi_{11}r) r^2 dr \quad (12)$$

From Eq. (10), we see that the exciton energy spectrum in the presence of a pump laser consists of four levels, in which two levels E_{10}^+ and E_{10}^- are separated from the level E_{10} , and two levels E_{11}^+ and E_{11}^- are separated from the

level E_{11} (Fig. 3). These separated levels are defined as

$$\begin{cases} E_{10}^- = E_{10} - \hbar\alpha_2 \\ E_{10}^+ = E_{10} + \hbar\alpha_1 \end{cases}, \quad (13)$$

and

$$\begin{cases} E_{11}^- = E_{11} - \hbar\alpha_1 \\ E_{11}^+ = E_{11} + \hbar\alpha_2 \end{cases}. \quad (14)$$

From Eqs. (11), (13) and (14), we have

$$\begin{cases} E_{10}^+ - E_{10}^- = 2\hbar\Omega_R \\ E_{11}^+ - E_{11}^- = 2\hbar\Omega_R \end{cases}. \quad (15)$$

From Eq. (15), we see that the energy difference between two split levels E_{10}^- and E_{10}^+ or E_{11}^- and E_{11}^+ is equal to $2\hbar\Omega_R$ (Ω_R is the Rabi frequency determined in Eq. (11)).

2.2 The absorption intensity of exciton in the absence of a pump laser

In this section, we determine the time-dependent absorption intensity of exciton through the optical transition matrix element between exciton levels in the absence of the pump laser. According to the selection rule for optical transitions in quantum dot structures, the transitions can only occur between the ground state corresponding to E_{ground} level and the first excited state corresponding to E_{10} level of the exciton. Therefore, under the effect of a probe laser, the transition matrix element between these two levels is determined as follows

$$T_{10}^{Ex} = \langle \Lambda_{10}(\vec{r}, t) | \hat{H}_{int} | 0 \rangle. \quad (16)$$

Substituting Eqs. (1) and (7) into Eq. (16), we finally get the transition matrix element expression T_{10}^{Ex} as follows

$$T_{10}^{Ex} = -\frac{qA_t}{m_0 i\omega_t} e^{\frac{i}{\hbar} E_{10} - \hbar\omega_t t} p_{cv} \langle \Psi_{10}^e(\vec{r}) \Psi_{10}^h(\vec{r}) | 0 \rangle, \quad (17)$$

where $p_{cv} = \langle u_c \vec{r} | \vec{n}\hat{p} | u_v \vec{r} \rangle$ is the polarization matrix element between the conduction and valence bands.

From that, we can find the expression of the absorption intensity of exciton in the absence of the pump laser by making use of the following relation

$$I_{10}^{Ex}(t) \propto |T_{10}^{Ex}|^2. \quad (18)$$

Substituting Eq. (17) into Eq. (18) and inputting the damped factor $\exp -\gamma t$ phenomenologically, with $\gamma = 1 / T_1$ (T_1 is the lifetime of the exciton on the first excitation), we finally obtain the intensity absorption of exciton as follows

$$I_{10}^{Ex}(t) \propto |T_{10}^{Ex}|^2 = \left(\frac{qA_t p_{cv}}{m_0 \omega_t} \right)^2 \exp -\gamma t. \quad (19)$$

2.3 The absorption intensity of exciton in the presence of a pump laser

When the system is irradiated by a probe laser under the influence of a short pump laser with a frequency close to the difference between the two quantization energy levels of the electron, the excitons exist in the mixed state described by the wave function shown in Eq. (10). Therefore, the transition matrix element between the ground state and the mixed state $|\Lambda_{mix}(\vec{r}, t)\rangle$ of the exciton is determined as follows

$$T_{mix}^{Ex} = \langle \Lambda_{mix}(\vec{r}, t) | \hat{H}_{int} | 0 \rangle. \quad (20)$$

Substituting Eqs. (7) and (10) into Eq. (20) and applying the selection rule for optical transitions in the quantum dot structure, the absorption intensity expression in equation (20) can be rewritten as follows

$$T_{mix}^{Ex} = -\frac{qA_t p_{cv}}{m_0 \omega_t} \frac{1}{2\Omega_R} \left(\alpha_1^* e^{i(E_{10}^- - \hbar\omega_t)t} + \alpha_2^* e^{i(E_{10}^+ - \hbar\omega_t)t} \right) \times \langle \Psi_{10}^e(\vec{r}) \Psi_{10}^h(\vec{r}) | 0 \rangle \quad (21)$$

According to Eq. (15), the energy separation between two levels E_{10}^- and E_{10}^+ is $2\hbar\Omega_R$, so to be able to excite two excitons in E_{10}^-, E_{10}^+ pair simultaneously, the spectral width of the probe pulse must be greater than $2\hbar\Omega_R$. Besides, the pulse duration of the probe laser must be shorter than the coherence time T_2 of the non-stationary state of the exciton (determined in Eq. (10)) to keep this state being coherent. At any time $t < T_2$, the absorption intensity of the exciton $I_{mix}^{Ex} t$ is determined as follows

$$I_{mix}^{Ex} t \propto |T_{mix}^{Ex}|^2 = \left(\frac{qA_t p_{cv}}{m_0 \omega_t} \right)^2 \times \left[\beta_1^2 + \beta_2^2 + 2\beta_1 \beta_2 \cos 2\Omega_R t \right], \quad (22)$$

where

$$\begin{cases} \beta_1 = \frac{\alpha_1}{2\Omega_R}, \\ \beta_2 = \frac{\alpha_2}{2\Omega_R}. \end{cases} \quad (23)$$

In practice, however, the superposition states described in Eq. (10) decay over time. Therefore, in order to observe the damping of the absorption intensity $I_{mix}^{Ex} t$ we can phenomenologically introduce the damped factors $\exp -\gamma t$ and $\exp -\tau t$ with $\gamma = 1 / T_1$ and $\tau = 1 / T_2$, the absorption intensity of the exciton under the affection of a pump laser can be obtained as follows

$$I_{mix}^{Ex} t = \left(\frac{qA_t p_{cv}}{m_0 \omega_t} \right)^2 \left[\beta_1^2 + \beta_2^2 \exp -\gamma t + 2\beta_1 \beta_2 \exp -\tau t \cos 2\Omega_R t \right]. \quad (24)$$

3 The numerical results and discussion

In this work, we investigate the quantum beat through the formula of the exciton absorption intensity in two cases: with and without the influence of a pump laser, which are determined

in Eqs. (19) and (24). The numerical calculations are performed on a typical GaAs/AlAs disk-shaped quantum dot with the corresponding material parameters given as follows: $m_e^* = 0.067m_0$ and $m_h^* = 0.51m_0$ are the electron and hole effective masses, respectively; $E_g = 1424$ meV is the band-gap energy of the material, and $\Gamma = 0.1$ meV is the linewidth.

As seen in Fig. 4, we start by examining the time-dependent exciton absorption intensity in a disk-shaped quantum dot with the dot radius $R = 50$ Å and the detuning $\hbar\Delta\omega = 0$ meV in both the presence and absence of a pump laser. This graph demonstrates that the exciton absorption intensity is a smooth curve (dashed line) that gradually diminishes to zero in the absence of the pump laser, demonstrating that the quantum beat is not created. On the other hand, when the system is exposed to a powerful resonant pump laser, the exciton absorption intensity grows as a periodic oscillation that decays with a constant frequency equal to twice the Rabi frequency (solid line). In other words, under the influence of a pump laser, the disk-shaped quantum dot revealed the quantum beat of an exciton.

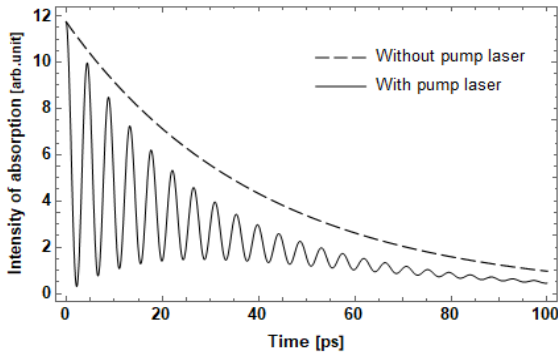


Fig. 5. The absorption intensity of exciton in GaAs/AlAs disk-shaped quantum dot with radius $R = 50$ Å in the absence of a pump laser (dashed line) and the presence of a pump laser with resonant detuning $\hbar\Delta\omega = 0$ meV (solid line)

Under the influence of a pump laser, the formation of quantum beats in the quantum dot is described as follows. Initially, in the absence of the pump laser, the system contained only two levels of electron, which correspond to four possible states according to the Pauli's exclusion principle. When the system is then irradiated by a powerful pump laser, the two initial electron levels are combined to produce a uniform level. According to Pauli's exclusion principle, only two states are permitted on this uniform level. For the system's number of possible states to remain at four, each initial electron level must be subdivided into two sublevels, that is, level E_{10}^e splits into E_{10}^{e+} and E_{10}^{e-} , while level E_{11}^e splits into E_{11}^{e+} and E_{11}^{e-} . Thus, two excitons with closed energies are generated when the system is exposed to an appropriate probe laser with a linewidth larger than $2\hbar\Omega_R$, which is the energy difference between two split levels E_{10}^- and E_{10}^+ . In addition, because these two excitons are in phase, their interference will produce exciton quantum beats as expected.

Next, we investigate the effect of the geometric parameters of the quantum dot and the pump laser field on the absorption intensity of the exciton to examine in depth the behavior of the quantum beat. Fig. 5 illustrates the effect of dot

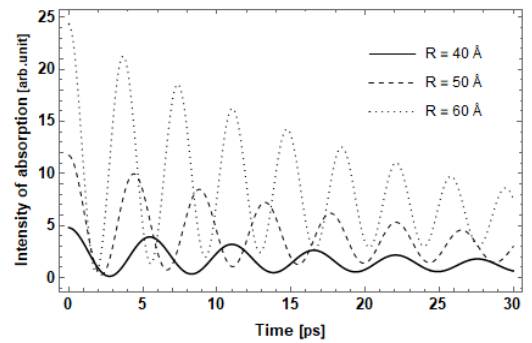


Fig. 4. The time-dependent absorption intensity of the exciton in the disk-shaped quantum dot under the action of a pump laser with the resonant detuning $\hbar\Delta\omega = 0$ meV corresponding to three different values of the radius: $R = 40$ Å (solid line), $R = 50$ Å (dashed line) and $R = 60$ Å (dotted line)

radius R on the time-dependent absorption intensity of exciton under the pump laser with detuning $\hbar\Delta\omega = 0$ meV. This figure demonstrates that the absorption intensity oscillates over time and that the radius of the quantum dot strongly influences its oscillating characteristics. This further verifies the existence of the exciton quantum beat in the disk-shaped quantum dot. In addition, the figure reveals that as the radius of the quantum dot increases, the period of the beat decreases while the amplitude of the beat increases. This implies that the quantum beat occurs quicker and with greater intensity as the dot radius increases.

The reasons for these features are that with the increasing of R , the interval between the two quantization levels of the electron decreases, making them closer to each other. So under the action of the pump laser, these two levels are easily paired together to form a single level. Therefore, to satisfy the Pauli's exclusion principle, the initial levels of electrons must be separated to new levels that are twice as many as the original ones. Then, when the system is irradiated by a suitable probe laser, we will observe the transitions from the hole level to the electron separation levels. Thus, excitons with close energy are rapidly created, causing the quantum beats to be formed quickly. Furthermore, the probe laser frequency is a decreased function of the quantum dot radius. According to Eq. (24), the absorption intensity of the exciton is inversely proportional to the probe laser frequency, so an increase in the dot radius leads to increment of the beat amplitude. In addition, according to Eq. (11), the Rabi frequency Ω_R is proportional to the intraband transition matrix element V_{10} between the two initial levels of the electron. On the other hand, according to Eq. (12), this matrix element increases with the dot radius. Therefore, as the dot radius increases, the Rabi frequency Ω_R also increases, leading to an

increment in the beat frequency or a decrement in the beat period because the beat frequency is twice the Rabi frequency.

Next, we investigate the influence of the pump laser detuning on the time-dependent absorption intensity of the exciton in the quantum dot with $R = 60$ Å shown in Fig. 6. From the figure, we can see that as the detuning increases, the oscillation amplitude decreases. It is clear that when the detuning increases, the two levels of electrons are more difficult to pair, leading to a decrease in the splitting ability of the electron levels as well as the formation of two close-energy excitons. It will reduce the probability of quantum beat formation and ultimately reduce the amplitude of the beat.

To elucidate the characteristics of the beat period, we investigated the effect of the radius of the quantum dot on the beat period for various detuning values (Fig. 7). As both the detuning and

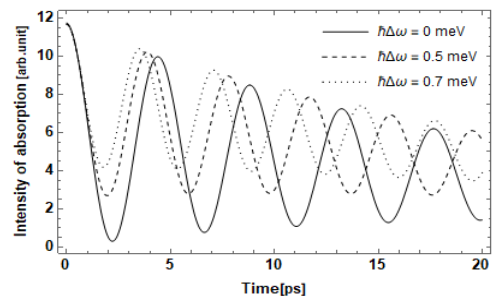


Fig. 6. The time-dependent absorption intensity of the exciton in a disk-shaped quantum dot with different detunings $\hbar\Delta\omega = 0$ meV (solid line), $\hbar\Delta\omega = 0.5$ meV (dashed line) và $\hbar\Delta\omega = 0.7$ meV (dotted line) and the radius $R = 60$ Å

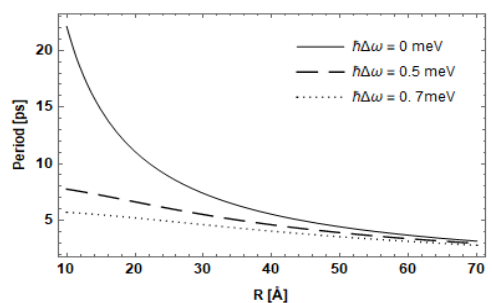


Fig. 7. The dependence of the quantum beat period on the quantum dot radius and the pump laser detuning

the radius of the quantum dot increase, the beat period decreases (or beat frequency increases). As the radius of the quantum dot increases, the beat period in all three instances tends to approach the same value.

4 Conclusion

In this study, we used the renormalized wavefunction approach to examine the properties of the exciton quantum beat in a GaAs/AlAs disk-shaped quantum dot covered by an infinite potential. The numerical studies have showed that, in the presence of a resonant pump laser, the time-dependent exciton absorption intensity takes the shape of a damped oscillation with a frequency equal to twice the electron Rabi frequency. This demonstrates the presence of the exciton quantum beat in the disk-shaped quantum dot. Additionally, the quantum beat forms more quickly and with a higher oscillation frequency as the dot radius increases. On the other hand, as resonant detuning increases, the amplitude and period of the quantum beat tend to decrease. Last but not least, we expect that the data can help future experimental research on the quantum beat of excitons.

Acknowledgement

This work is supported by Hue University under Grant No. DHH2021 - 01 – 191.

References

1. Lv Z, Wang Y, Chen J, Wang J, Zhou Y, and Han ST. Semiconductor Quantum Dots for Memories and Neuromorphic Computing Systems. *Chemical Reviews*.2020;120:3941-4006.
2. Nozik AJ, Beard MC, Luther JM, Law M, Ellingson RJ, Johnson JC. Semiconductor Quantum Dots and Quantum Dot Arrays and Applications of Multiple Exciton Generation to Third-Generation Photovoltaic Solar Cells. *Chemical Reviews*. 2010; 110:6873-6890.
3. Czajkowski G and Silvestri L. Optical properties of Quantum Disks: Real density matrix approach. *Central European Journal of Physics*. 2006;4:254-269.
4. Duque CM, Restrepo RL, Duque CA. Tilted electric field effects on the electronic states in a GaAs quantum disk. *Superlattices and Microstructures*. 2012;52:1078-1082.
5. Liu G, Guo K, Wang C. Linear and nonlinear intersubband optical absorption in a disk-shaped quantum dot with a parabolic potential plus an inverse squared potential in a static magnetic field. *Physica B: Condensed Matter*. 2012;407:2334-2339.
6. Wei R, Xie W. Optical absorption of a hydrogenic impurity in a disc-shaped quantum dot. *Current Applied Physics*. 2010;10:757-760.
7. Xie W. Exciton states in a disk-like quantum dot. *Physica B: Condensed Matter*. 2000;279:253-256.
8. Chen CY, Li WS, Teng XY, Liang SD. Polaron in a quantum disk. *Physica B: Condensed Matter*. 1998; 245:92-102.
9. Van der Poel WAJA, Severens ALGJ, Foxon CT. Quantum beats in the exciton emission of type II GaAs/AlAs quantum wells. *Optics Communications*. 1990;76:116-120.
10. Nuss MC, Planken PCM, Brener I, Roskos HG, Luo MSC, Chuang SL. Terahertz electromagnetic radiation from quantum wells. *Applied Physics B Laser and Optics*. 1994;58:249-259.
11. Planken PCM, Nuss MC, Brener I, Goossen KW, Luo MSC, Chuang SL, Pfeiffer L. Terahertz emission in single quantum wells after coherent optical excitation of light hole and heavy hole excitons. *Physical Review Letters*. 1992;69:3800-3803.
12. Kojima O, Miyagawa A, Kita T, Wada O, Isu T. Ultrafast All-Optical Control of Excitons Confined in GaAs Thin Films. *Applied Physics Express*. 2008;1(11):112401.
13. Haroche S. Quantum beats and time-resolved fluorescence spectroscopy. *High-Resolution Laser Spectroscopy*. 1976;253-313.
14. Pantke KH, Schillak P, Erland J, Lyssenko VG, Razbirin BS, Hvam JM. Nonlinear Quantum Beats

- of Excitons in CdSe. *Physica Status Solidi (b)*. 1992;173:91-98.
15. Luo MSC, Chuang SL, Planken PCM, Brener I, Nuss MC. Coherent double-pulse control of quantum beats in a coupled quantum well. *Physical Review B*. 1993;48:11043-11050.
 16. Bobrysheva AI, Shmiglyuk MI, Pavlov VG. Optical exciton Stark effect and quantum beats at exciton quasienergy levels in quantum wells. *Physics of the Solid State*. 1997;39:1147-1149.
 17. Thao DN, Bao LTN. Quantum Beat of Excitons in Spherical Semiconductor Quantum Dots. *Superlattices and Microstructures*. 2020;146:106675.
 18. Phuoc DD, Bao LTN, Hien LTD, Hieu HK, Thao DN. A Study on Quantum Beats of Excitons in GaAs/AlGaAs Circular Cylindrical Quantum Wires. *Japanese Journal of Applied Physics*. 2020; 59:125003.
 19. Bao LTN, Phuoc DD, Hien LTD, Thao DN. Quantum Beats of Excitons in the Prolate Ellipsoidal Quantum Dots. *Journal of Nanomaterial*. 2022; 2022:1-14.
 20. Sangalli D, Perfetto E, Stefanucci G, and Marini A. An ab-initio approach to describe coherent and non-coherent exciton dynamics. *The European Physical Journal B*. 2018;91:171.
 21. Rustagi A, Kemper AF. Coherent excitonic quantum beats in time-resolved photoemission measurements. *Physical Review B*. 2019;99:125303.